CONSEQUENCES OF LONGITUDINAL COUPLED-BUNCH INSTABILITY MITIGATION ON POWER REQUIREMENTS DURING THE HL-LHC FILLING

I. Karpov*, P. Baudrenghien, L. E. Medina Medrano, H. Timko, CERN, Geneva, Switzerland

Abstract

During the filling of the Large Hadron Collider (LHC), it is desirable to keep the RF cavity voltage constant both in amplitude and phase to minimize the emittance blow-up and injection losses. To have a constant voltage and to minimize power consumption, a special beam-loading compensation scheme called half-detuning is used in the LHC, for which the cavity fundamental resonant frequency needs to be detuned from the RF frequency by an appropriate value. This, however, can result in fast coupled-bunch instabilities caused by the asymmetry of the fundamental cavity impedance. To mitigate them, a fast direct RF feedback and a one-turn delay feedback are presently used in the LHC. The semi-analytical model that describes the dynamics of the Low-Level RF system in the LHC shows that, depending on the mitigation scenario, the required transient RF power during injection could significantly exceed the steady-state value. This means that for High-Luminosity LHC (HL-LHC) beam intensities, one can potentially reach the limit of available RF power. In this paper, the model is described, and benchmarks with LHC measurements are presented. We also shortly revisit the damping requirements for the longitudinal coupled-bunch instability at injection energy, to find a compromise between longitudinal stability and RF power requirements for the HL-LHC beam.

INTRODUCTION

During the filling of the Large Hadron Collider (LHC), it is desirable to reduce RF power requirements and to minimize the emittance blow-up and injection losses. This can be achieved if half-detuning beam loading compensation scheme is used [1], which keeps the RF cavity voltage constant both in amplitude and phase. Detuning causes asymmetry of the fundamental cavity impedance, which can drive longitudinal coupled-bunch instabilities. In the LHC, they are mitigated by a direct RF feedback [2] and a one-turn delay feedback (OTFB) [3] which reduce the impedance seen by the beam and defined as the closed-loop impedance

$$Z_{\mathrm{cl}}(\omega) = \frac{Z(\omega)}{1 + e^{-i\tau_{\mathrm{delay}}\omega} G(\omega) Z(\omega)}. \tag{1}$$

Here, Z is the RF cavity impedance, τ_{delay} is the loop delay, and G is the frequency dependent gain. The feedback can reduce the impedance at frequencies where the absolute value of the denominator is significantly larger than 1.

In steady-state operation, feedbacks do not require significant additional power to suppress longitudinal coupled-bunch instabilities. Operational experience, however, suggests that power transients between beam- and no-beam segments need to be included in the analysis [4]. In the present work, we evaluate RF power transients during the injection process. If there is a large power overshoot, one can potentially reach the limit of the available RF power in the klystrons (about 300 kW [5]) for High-Luminosity LHC (HL-LHC) requiring higher-intensity beams.

* ivan.karpov@cern.ch

BEAM-GENERATOR-CAVITY INTERACTION MODEL

To evaluate power transients during the injection process in the LHC, the present work extends the description of beam-generator-cavity interaction [6] taking into account the details of the Low-Level RF (LLRF) system in the LHC [5] (see Fig. 1). The LHC employs superconducting cavities which are connected to generators (klystrons) via circulators, so that the whole reflected current (I_r) is absorbed in a load. The RF voltage V is defined by the RF component of the beam current $I_{b,\mathrm{RF}}$ and the generator current I_g fed into the cavity via a main coupler [6]:

$$I_g(t) = \frac{V(t)}{2(R/Q)}\left(\frac{1}{Q_L} - 2i\frac{\Delta\omega}{\omega_{\mathrm{RF}}}\right) + \frac{dV(t)/dt}{\omega_{\mathrm{RF}}(R/Q)} + \frac{I_{b,\mathrm{RF}}(t)}{2}. \tag{2}$$

Here $(R/Q) = 45\,\Omega$, $\Delta\omega = \omega_r - \omega_{\mathrm{RF}}$ is the cavity detuning, $f_r = \omega_r/2\pi$ is the cavity resonant frequency, $\omega_{\mathrm{RF}} = 2\pi f_{\mathrm{RF}} = 2\pi h f_0$, $f_{\mathrm{RF}} = 400.79$ MHz is the RF frequency, $f_0 = 1/T_0$ is the revolution frequency, T_0 is the revolution period, and $h = 35640$ is the harmonic number. The loaded quality factor $Q_L = (1/Q_{\mathrm{ext}} + 1/Q_0)^{-1}$ is calculated from the cavity quality factor Q_0 and the coupler quality factor $Q_{\mathrm{ext}} = Z_c/(R/Q)$ defined by Z_c, the line impedance transformed to the gap by the main coupler. For a superconducting cavity with $Q_0 \gg Q_{\mathrm{ext}}$, $Q_L \approx Q_{\mathrm{ext}}$. Note that in Eq. (2) V, $I_{b,\mathrm{RF}}$ and I_g are the complex phasors and the corresponding phases are chosen such that in the absence of the beam the cavity voltage is real.

Equation (2) allows to treat the case when $I_{b,\mathrm{RF}}$ is modulated due to the gaps in the ring filling. In reality, the RF power chain (klystron, circulator, etc.) has limited bandwidth and cannot track the fast bunch-by-bunch variations of the beam current. In addition, the synchronous clock is used for processing in the LHC with a sampling time corresponding to the bunch spacing of $t_{\mathrm{bb}} = 10\ t_{\mathrm{RF}}$, where $t_{\mathrm{RF}} = 1/f_{\mathrm{RF}}$ is the RF period. In what follows, time is discretized with a the sampling frequency $f_{\mathrm{bb}} = 1/t_{\mathrm{bb}}$. We use a function u, which describes the filling scheme. It is defined on $h/10$ sampling points per turn, $u = 1$ in the filled buckets, and

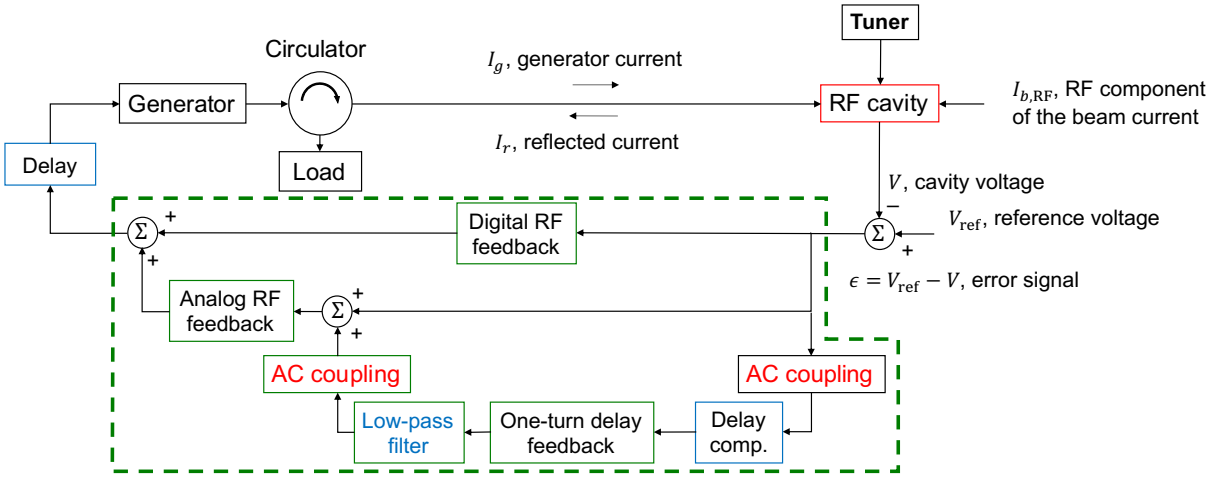

Figure 1: Beam-generator-cavity interaction model. The elements inside the dashed contour are the part of the low-level RF system.

$u = 0$ in the gaps. Thus, the RF component of the beam current in Eq. (2) is

$$I_{b,\mathrm{RF}}(t) = i\frac{eN_pF_b}{t_{\mathrm{bb}}}u(t)e^{i\phi_b(t)} = i\hat{I}_{b,\mathrm{RF}}e^{-i\phi_s+i\phi_b(t)}u(t), \tag{3}$$

where $\hat{I}_{b,\mathrm{RF}} = |F_b|eN_p/t_{\mathrm{bb}}$, N_p is the number of particles per bunch, ϕ_s is the average bunch position, and ϕ_b is the bunch-by-bunch phase modulation. The complex form factor [7]

$$F_b = 2\frac{\mathcal{F}\left[\lambda(t)\right]_{\omega=\omega_{\mathrm{RF}}}}{\mathcal{F}\left[\lambda(t)\right]_{\omega=0}} = |F_b|e^{-i\phi_s} \tag{4}$$

is obtained from the bunch profile λ as the ratio of the Fourier transform of λ at the RF frequency to λ at DC. It depends on the particle distribution function [8]. For symmetric Gaussian bunches with rms bunch length σ, the magnitude of the form factor can be approximated as $|F_b| \approx 2\exp\left[-(\omega_{\mathrm{RF}}\sigma)^2/2\right]$ and ϕ_s is the same as the synchronous phase.

The generator current in Eq. (2) depends on detailed implementation of the LLRF loops which are described in the following subsections. For each element, the transfer function H is defined as

$$H(s) = \frac{Y(s)}{X(s)}$$

in Laplace notation, with the complex variable s, the input signal being X, and the output signal being Y. Note that $s = i(\omega - \omega_{\mathrm{RF}})$ is related to the angular frequency ω, so that the LLRF response is centered at ω_{RF}. In the past, a part of the model was developed using MATLAB and Simulink software packages [9]. At present, two similar implementations (stand-alone and in the BLonD particle tracker suite [10]) are available in Python. The corresponding transfer functions are replaced by their discrete time-domain forms in the codes and solved together with Eq. (2) using the Euler method. The LLRF loops act on the error signal ϵ (difference between the actual value V and the reference value V_{ref} of the cavity voltage) to control the RF voltage in the cavity.

Finally, to evaluate the time evolution of the RF power, the following equation is used [6]

$$P(t) = \frac{1}{2}(R/Q)Q_{\mathrm{ext}}|I_g(t)|^2 \approx \frac{1}{2}(R/Q)Q_L|I_g(t)|^2. \tag{5}$$

Direct RF feedback

The LHC direct RF feedback consists of two branches: the analog and the digital paths. They can be described by a transfer function as the sum of high-pass and low-pass filters in Laplace notation

$$H_{a,d}(s) = G_a\frac{\tau_a s}{1+\tau_a s} + G_d\frac{1}{1+\tau_d s}, \tag{6}$$

where G_a is the gain of the high-pass filter, τ_a is the high-pass filter time constant, G_d is the gain for the low-pass filter, and τ_d is the time constant of the low-pass filter. While in the presence of the analog RF feedback, the closed-loop impedance is smaller than the cavity impedance, the digital RF feedback ensures precise control of the static cavity voltage amplitude and phase due to a higher gain ($G_d > G_a$) in the low-frequency range, $|f - f_r| < f_0$. In the LHC, the following values are used in operation: $\tau_a = 170\,\mu\mathrm{s}$, $\tau_d = 400\,\mu\mathrm{s}$, $G_d = 10\ G_a$, and $G_a = G_a^m = 6.79\times10^{-6}\ 1/\Omega$ is chosen to obtain a flat closed-loop response H_{cl} for loop delay of $\tau_{\mathrm{delay}} = 650\,\mathrm{ns}$,

$$G_a^m = \frac{1}{2(R/Q)\omega_{\mathrm{RF}}\tau_{\mathrm{delay}}},$$

where the closed-loop transfer function is defined as

$$H_{\mathrm{cl}}(s) = \frac{2e^{-\tau_{\mathrm{delay}}s}H_{a,d}(s)Z(s)}{1+2e^{-\tau_{\mathrm{delay}}s}H_{a,d}(s)Z(s)}. \tag{7}$$

The factor of 2 in Eq. (7) is coming from the fact that the transfer function from I_g to V based on Eq. (2) is twice the RF cavity impedance $Z(s)$, which is approximated as

$$Z(s) = \frac{(R/Q)Q_L}{1+2Q_L(s-i\Delta\omega)/\omega_{\mathrm{RF}}}.$$

One-turn delay feedback

An additional means to reduce the closed-loop impedance is to use OTFB. In the LHC, the input and output signals of the OTFB branch are AC-coupled, so there is no influence on the average voltage in the cavity. The transfer function of the AC-coupling is

$$H_{\mathrm{AC}}(s) = \frac{\tau_{\mathrm{AC}} s}{1+\tau_{\mathrm{AC}} s}\,, \tag{8}$$

with the time constant $\tau_{\mathrm{AC}} = 110\,\mu\mathrm{s}$. The OTFB response is modeled as a comb filter [2]

$$H_{\mathrm{OTFB}}(s) = G_{\mathrm{OTFB}}\frac{(1-a_{\mathrm{OTFB}})e^{-(T_0-\tau_{\text{delay comp}})s}}{1-a_{\mathrm{OTFB}}e^{-T_0 s}}\,, \tag{9}$$

where $G_{\mathrm{OTFB}} = 10$ is the OTFB gain, $a_{\mathrm{OTFB}} = 15/16$ is the constant defining the bandwidth of the resonances, and $\tau_{\text{delay comp}}$ is an adjustable delay that compensates for the delay of the closed-loop response defined in Eq. (7). In the LHC, $\tau_{\text{delay comp}} \approx 1.2\,\mu\mathrm{s}$ is used, while it will be shown below that this delay affects the evolution of RF power transients during the injection process.

Finally, a symmetric, finite-impulse response (FIR) filter is used to control (and limit) the OTFB bandwidth. The transfer function of this low-pass filter (LPF) is

$$H_{\mathrm{LPF}}(s) = e^{(N_{\mathrm{tap}}-1)t_{\mathrm{bb}}s/2}\sum_{k=0}^{N_{\mathrm{tap}}-1} b_k e^{-k t_{\mathrm{bb}} s}, \tag{10}$$

where N_{tap} is the number of taps of the FIR filter ($N_{\mathrm{tap}} = 63$ in the LHC), and the filter coefficients b_k are listed in the Appendix.

Apart from stabilising the beam, the feedback loops provide also transient beam-loading compensation. The particular compensation scheme that is used during the injection process in the LHC is described in the following section.

HALF-DETUNING SCHEME

To keep the cavity voltage amplitude and phase constant ($V(t) = V_{\mathrm{cav}} = \text{constant}$), the feedback loops will try to compensate the beam-induced voltage. For a non-uniform filling of the ring, the steady-state RF power in this scheme is at its minimum and is the same in beam and no-beam segments if the following frequency detuning and loaded quality factor are used [1]

$$\Delta\omega_{1/2} = -\omega_{\mathrm{RF}}\frac{\hat{I}_{b,\mathrm{RF}}(R/Q)}{4V_{\mathrm{cav}}},\quad Q_{L,1/2} = \frac{2V_{\mathrm{cav}}}{(R/Q)\hat{I}_{b,\mathrm{RF}}}. \tag{11}$$

The corresponding steady-state power is

$$P_{\mathrm{th}} = \frac{V_{\mathrm{cav}}\hat{I}_{b,\mathrm{RF}}}{8}. \tag{12}$$

During Run I and Run II operation, the RF power at injection was typically around 100 kW and the main coupler was not adjusted to minimise the RF power, but rather to be at a constant working point corresponding to $Q_L = 20000$ during injection. The cavity was detuned automatically after beam injection using the algorithm described below.

Tuning algorithm

To optimize the RF power requirements in steady-state operation, a cavity detuning algorithm was proposed and implemented in the LHC [11]. The cavity detuning changes between consecutive turns n and $n+1$ as

$$\left(\frac{\Delta f}{f_0}\right)_{n+1} = \left(\frac{\Delta f}{f_0}\right)_n - \frac{\mu}{2}\frac{\mathrm{Im}\left[VI_g\right]_{\mathrm{min}} + \mathrm{Im}\left[VI_g\right]_{\mathrm{max}}}{|V_{\mathrm{cav}}|^2}, \tag{13}$$

where μ sets the rate of convergence with a time constant of the detuning process in the order of a second. The quantities in the square brackets are down-sampled using a Cascaded-integrator–comb (CIC) filter with the following transfer function

$$H_{\mathrm{CIC}}(s) = \frac{1}{64}\left(\frac{1-e^{-8t_{\mathrm{bb}}s}}{1-e^{-t_{\mathrm{bb}}s}}\right)^2, \tag{14}$$

and then $\mathrm{Im}\left[VI_g\right]_{\mathrm{min}}$ and $\mathrm{Im}\left[VI_g\right]_{\mathrm{max}}$ are obtained within one turn. In our model, the tuner model was implemented together with the direct RF feedback and OTFB, and it was benchmarked with measurements in the steady-state case, which is described in the following subsection.

Comparison with measurements in steady-state

The half-detuning scheme was employed during the whole LHC cycle until 2014. The modulations of the generator forward power, the generator current phase, the cavity voltage amplitude, and the cavity voltage phase measured at 6.5 TeV with a full machine are shown in Fig. 2 (measured data from Ref. [12]). The modulation pattern is defined by gaps in the filling scheme: 225 ns due to the Super Proton Synchrotron (SPS) injection kicker rise time, 900 ns due to the LHC injection kicker rise time, and finally 6.85 µs due to the LHC abort gap. There were 2244 bunches (36 bunches in the Proton Synchrotron (PS) batches, either one, three or four PS batches per SPS batch) circulating in the machine with the average bunch intensity of $N_p = 1.2\times10^{11}$ protons per bunch (p/b) and a bunch length of about 1 ns ($|F_b| = 1.64$). We used the implemented LLRF and tuner models to evaluate the modulations for the same parameters (red dashed lines in Fig. 2).

The tuning algorithm in the model results in $\Delta\omega = 0.935\times\Delta\omega_{1/2}$, which is close to the theoretically predicted value of -4.6 kHz. In the steady-state situation, the model takes also into account that the bunch-by-bunch phase modulation follows the cavity phase modulation, so that the stable phase for all bunches is 180°. In general, we see that calculations reproduce well the measured modulations for $\tau_{\text{delay comp}} = 1175$ ns, while the measured value of the delay is not available in Ref [12]. Another uncertainty is the exact value of the cavity detuning in measurements. Note also that the corresponding steady-state power is $P_{\mathrm{th}} \approx 200$ kW [see Eq. (12)] in this case, while the peak power reaches more than 280 kW both in calculations and in measurements. This means, that Eq. (12) does not include the power transients caused by the transitions between beam and no-beam seg-

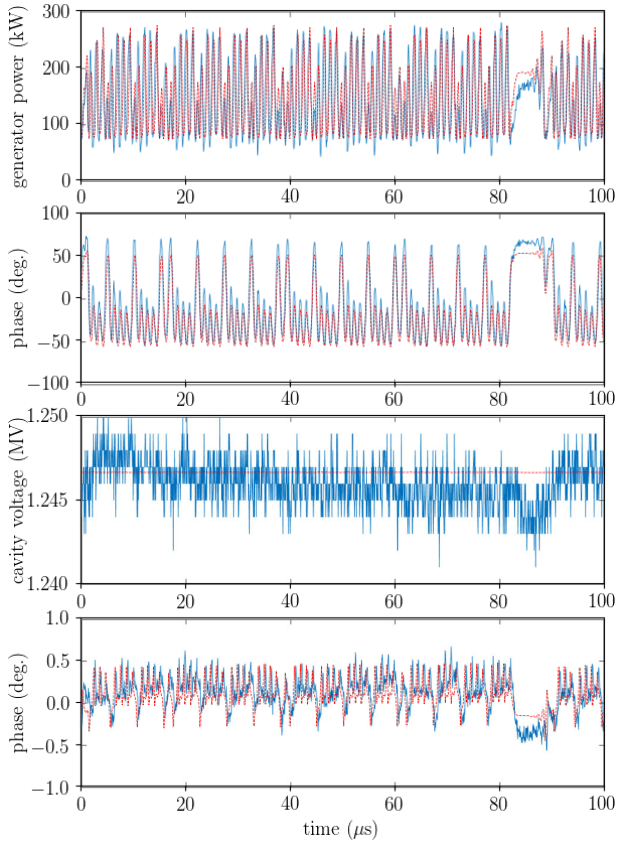

Figure 2: Comparison of generator forward power, generator current phase, cavity voltage amplitude, and cavity voltage phase (from top to bottom) from measurements (solid blue lines) and calculations using the developed model (red dashed lines). The plots are obtained by the overlap of the calculations with the data from Ref [12]. The modulations in the signals along the ring are due to beam-current modulations between batches. The beam and LLRF parameters are 2244 bunches, $N_p = 1.2 \times 10^{11}$ p/b, $\tau_{4\sigma} = 4\sigma = 1$ ns, $V_{\rm cav} = 1.25$ MV, $Q_L = 60000$, $\Delta\omega = 0.935\Delta\omega_{1/2}$, $G_a = G_a^m$, $G_d = 10\ G_a$, and $G_{\rm OTFB} = 10$, and $\tau_{\rm delay\ comp} = 1175$ ns.

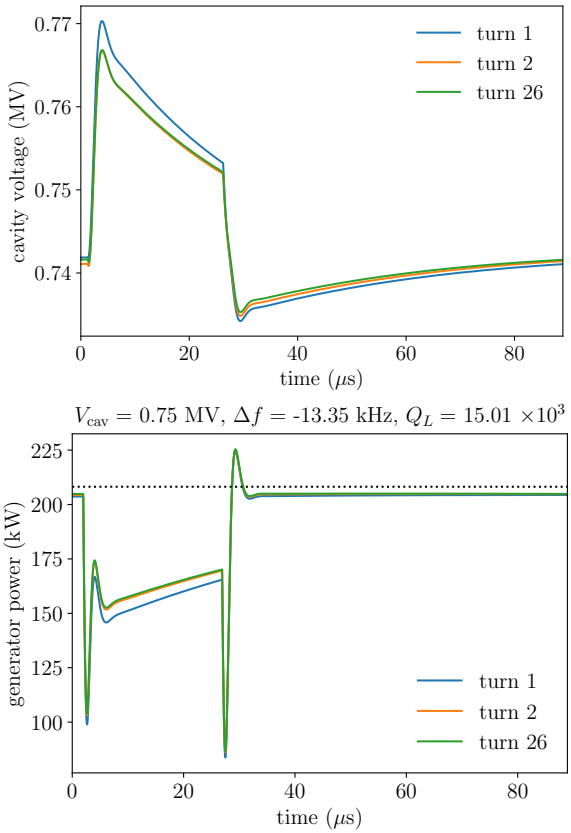

Figure 3: Cavity voltage amplitude (top) and RF power requirements (bottom) for selected turns after injection with the direct RF feedback on and the OTFB off. A beam without gaps is considered, with the first bunch at 1.3 μs and the last bunch at 26.3 μs. Parameters: $\hat{I}_{b,\rm RF} = 2.22$ A, $G_a = G_a^m$, $G_d = 10\ G_a$, and $G_{\rm OTFB} = 0$. The dashed line is the expected RF power in the steady-state [see Eq. (12)].

ments. In the next section we use the implemented model to evaluate the power transients during the injection process.

POWER EVOLUTION DURING INJECTION

The bunches extracted from the SPS 200 MHz main RF system are mismatched to the 400 MHz RF bucket of the LHC RF system, which results in their filamentation. In general, one has to model the dynamics of the interaction of the beam with the LLRF system in order to accurately evaluate transient effects. The present work focuses only on timescales which are shorter than the synchrotron period. This allows to assume that the beam parameters do not change during the calculation. In the cases presented below, a single batch of 1000 Gaussian bunches with $\tau_{4\sigma} = 4\sigma = 1.2$ ns ($|F_b| = 1.5$) and $N_p = 2.3 \times 10^{11}$ p/b (HL-LHC baseline) is injected into the LHC for $V_{\rm cav} = 0.75$ MV (6 MV of total RF voltage per beam) and different configurations of feedback loops. We also assume that the cavities are pre-detuned to the optimal frequency with beam loading and the quality factor is adjusted according to Eq. (11). In the following, the system of equations is initially solved for several tens of turns without beam to obtains steady-state conditions before injection and then the beam is taken into account in the calculations.

Case of direct RF feedback only

Considering the case when $G_a = G_a^m$ and the OTFB is switched off ($G_{\rm OTFB} = 0$), the modulations of the cavity voltage amplitude and of the RF power during the few first turns after injection are shown in Fig. 3. There is a small difference between traces due to a short time constant of its analog part defined by the physical loop delay $\tau_{\rm delay} = 650$ ns. A small difference between the first and the second turns comes from the action of the digital part of the direct RF feedback which has a time constant of several turns. The modulation of the cavity voltage amplitude in this case is of

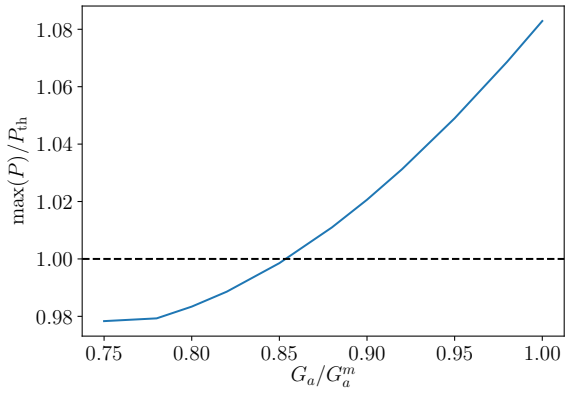

Figure 4: Normalized maximum needed RF power as a function of the direct RF feedback gain.

the order of 2-3 %. There is an overshoot in power in the no-beam segment behind the batch, which depends on the feedback gain (see Fig. 4). For $G_a < 0.85 G_a^m$, the power does not exceed the theoretical value [see Eq. (12)], but this might affect the longitudinal multi-bunch stability, since the closed-loop impedance will increase.

Case of direct RF feedback and OTFB

Similar calculations for the case with OTFB ($G_{\mathrm{OTFB}} = 10$) are shown in Fig. 5. The first turn after injection is the same as for the case without OTFB because of the one turn delay. The beam loading compensation from the OTFB takes several turns to develop due to its narrow bandwidth, resulting in a much smaller modulation of the cavity voltage after 26 turns. However, this comes at the expense of larger power transient at the batch head and after its tail, in comparison to the previous case. The power evolution depends on the adjustment of the delay in the OTFB branch: there is an overshoot either during transients or in the steady-state (see Fig. 6). The optimum delay is about 1100 ns, which corresponds to about 20 % excess in power, in short peaks of a few µs.

Considering the case of $G_a = 0.85\ G_a^m$ and $\tau_{\mathrm{delay\ comp}} = 1100$ ns, the peak power as a function of OTFB gain is shown in Fig. 7. For example, for $G_{\mathrm{OTFB}} \approx 5$ the power overshoot approximately corresponds to the one without OTFB and $G_a = G_a^m$. However, the use of the direct RF feedback alone will be less favorable for the beam stability as the compensation of the beam-induced voltage is reduced.

According to Ref. [13], for $V_{\mathrm{cav}} = 0.75$ MV (6 MV of total RF voltage) and $\tau_{4\sigma} = 1$ ns at injection energy, there is a stability margin of almost a factor of 3 for the case of the direct RF feedback alone and a factor of 40 with additional impedance reduction by OTFB. Still, further optimization requires benchmarking the model with injection transients observed during measurements performed in 2018 [14]. Moreover, particle tracking simulations including beam losses are required to optimize the system for future intensities.

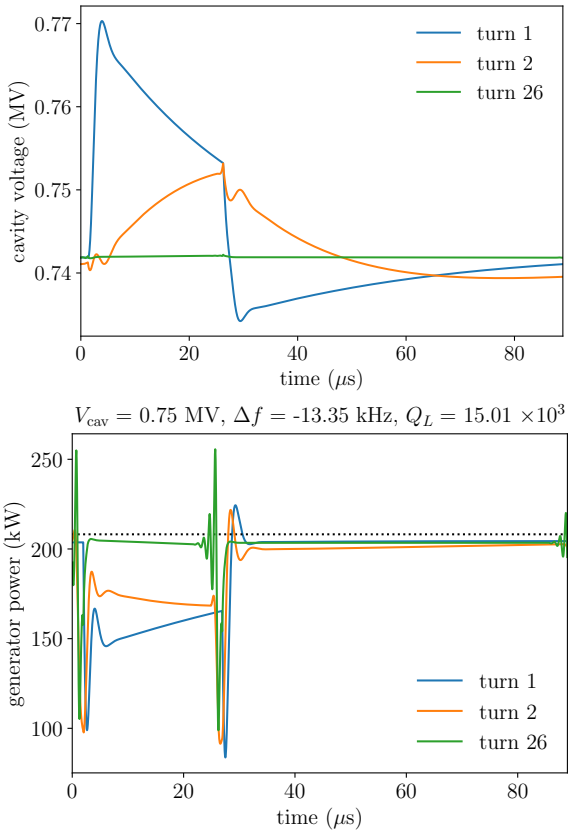

Figure 5: Cavity voltage amplitude (top) and RF power requirements (bottom) for selected turns after injection for HL-LHC parameters with both the direct RF feedback and OTFB on. The first bunch is at 1.3 µs and the last at 26.3 µs. Parameters: $\hat{I}_{b,\mathrm{RF}} = 2.22$ A, $G_a = G_a^m$, $G_d = 10\ G_a$, and $G_{\mathrm{OTFB}} = 10$, and $\tau_{\mathrm{delay\ comp}} = 1200$ ns. The dashed line is the expected RF power in the steady-state [see Eq. (12)].

SUMMARY

The LHC LLRF model was implemented using Python. It was benchmarked against measurements in steady-state condition and the comparison with power transients measured during injection is ongoing. Both the direct RF feedback and OTFB cause a power overshoot during the injection process in calculations and measurements. While power transients can be reduced by adjusting the feedback gains and the delay in the OTFB branch, there are potential consequences on beam stability. A more detailed analysis of coupled-bunch instability and possibly full beam dynamics simulations are still required to draw conclusions about the RF power requirement during the injection of HL-LHC beams.

ACKNOWLEDGEMENTS

We would like to thank Rama Calaga, Heiko Damerau, Wolfgang Höfle, John Molendijk, and Elena Shaposhnikova for useful comments and discussions.

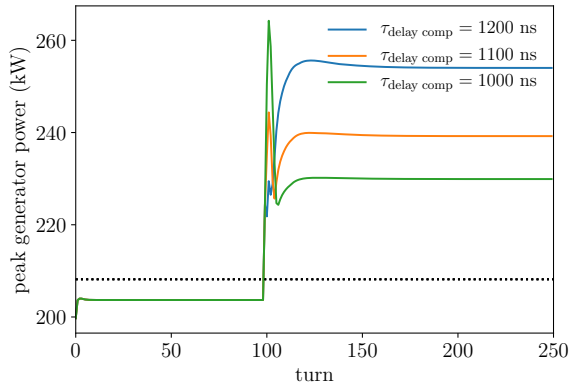

Figure 6: Evolution of the peak RF power for different delay compensations at injection. The first bunch is at 1.3 µs and the last at 26.3 µs. Parameters: $\hat{I}_{b,\text{RF}} = 2.22$ A, $G_a = G_a^m$, $G_d = 10\ G_a$, and $G_{\text{OTFB}} = 10$. Equations are solved without beam for the first 100 turns. The dashed line is the expected RF power in the steady-state [see Eq. (12)].

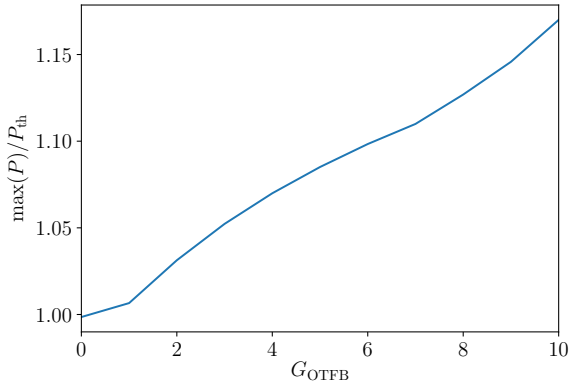

Figure 7: Normalized maximum needed RF power as a function of the OTFB gain for $G_a = 0.85\ G_a^m$ and $\tau_{\text{delay comp}} = 1100$ ns.

APPENDIX

The following coefficients of the FIR LPF [see Eq. (10)] are used in the LHC, b_k = [-0.038636, -0.00687283, -0.00719296, -0.00733319, -0.00726159, -0.00694037, -0.00634775, -0.00548098, -0.00432789, -0.00288188, -0.0011339, 0.00090253, 0.00321323, 0.00577238, 0.00856464, 0.0115605, 0.0147307, 0.0180265, 0.0214057, 0.0248156, 0.0282116, 0.0315334, 0.0347311, 0.0377502, 0.0405575, 0.0431076, 0.0453585, 0.047243, 0.0487253, 0.049782, 0.0504816, 0.0507121, 0.0504816, 0.049782, 0.0487253, 0.047243, 0.0453585, 0.0431076, 0.0405575, 0.0377502, 0.0347311, 0.0315334, 0.0282116, 0.0248156, 0.0214057, 0.0180265, 0.0147307, 0.0115605, 0.00856464, 0.00577238, 0.00321323, 0.00090253, -0.0011339, -0.00288188, -0.00432789, -0.00548098, -0.00634775, -0.00694037, -0.00726159, -0.00733319, -0.00719296, -0.00687283, -0.038636].

REFERENCES

[1] D. Boussard, "RF power requirements for a high intensity proton collider; parts 1 (chapters I, II, III) and 2 (chapters IV, V, VI)", CERN, Geneva, Switzerland, Rep. CERN-SL-91-16-RFS, May 1991.

[2] D. Boussard, "Control of cavities with high beam loading", IEEE Trans. Nucl. Sci., vol. 32, no. 5, pp. 1852–1856, 1985, doi:10.1109/TNS.1985.4333745.

[3] D. Boussard, G. Lambert, "Reduction of the apparent impedance of wide band accelerating cavities by RF feedback", IEEE Trans. Nucl. Sci., vol. 30, no. 4, pp. 2239-2241, 1983, doi:10.1109/TNS.1983.4332774.

[4] H. Timko, E. Shaposhnikova, K. Turaj, "Estimated LHC RF system performance reach at injection during Run III and beyond", CERN, Geneva, Switzerland, Rep. CERN-ACC-NOTE-2019-0005, Sep. 2018.

[5] O. Brüning *et al.*, "LHC design report vol.1: The LHC main ring", CERN, Geneva, Switzerland, Rep. CERN-2004-003, Jun. 2004.

[6] J. Tückmantel, "Cavity-beam-transmitter interaction formula collection with derivation", CERN, Geneva, Switzerland, Rep. CERN-ATS-Note-2011-002 TECH, Jan. 2011.

[7] P. F. Tavares, A. Andersson, A. Hansson, and J. Breunlin, "Equilibrium bunch density distribution with passive harmonic cavities in a storage ring", *Phys. Rev. ST Accel. Beams*, vol. 17, no. 6, p. 064401, Jun. 2014, doi:10.1103/PhysRevSTAB.17.064401.

[8] I. Karpov and P. Baudrenghien, "Transient beam loading and RF power evaluation for future circular colliders", *Phys. Rev. Accel. Beams*, vol. 22, no. 8, p. 081002, Aug. 2019, doi:10.1103/PhysRevAccelBeams.22.081002.

[9] J. Holma, "The model and simulations of the LHC 400 MHz cavity controller", CERN, Geneva, Switzerland, Rep. CERN-AB-2007-012, Feb. 2007.

[10] CERN beam longitudinal dynamics code BLonD, http://blond.web.cern.ch.

[11] P. Baudrenghien, "The tuning algorithm of the LHC 400 MHz superconducting cavities", CERN, Geneva, Switzerland, Rep. CERN-AB-2007-011, Feb. 2007.

[12] T. Mastoridis, P. Baudrenghien, and J. Molendijk, "Cavity voltage phase modulation to reduce the high-luminosity Large Hadron Collider RF power requirements", *Phys. Rev. Accel. Beams*, vol. 20, no. 10, p. 101003, Oct. 2017, doi:10.1103/PhysRevAccelBeams.20.101003.

[13] P. Baudrenghien and T. Mastoridis, "Fundamental cavity impedance and longitudinal coupled-bunch instabilities at the High Luminosity Large Hadron Collider", *Phys. Rev. Accel. Beams*, vol. 20, no. 1, p. 011004, Jan. 2017, doi:10.1103/PhysRevAccelBeams.20.011004.

[14] L. E. Medina Medrano *et al.*, "LHC MD 3165: RF power limitations at flat bottom", CERN, Geneva, Switzerland, Rep. CERN-ACC-NOTE-2019-0030, Jul. 2019.